EUROPEAN ORGANIZATION FOR NUCLEAR RESEARCH

CERN–PH–EP/2010–001
2 January 2010

The Spin-dependent Structure Function of the Proton g_1^p and a Test of the Bjorken Sum Rule

COMPASS Collaboration

Abstract

The inclusive double-spin asymmetry, A_1^p, has been measured at COMPASS in deep-inelastic polarised muon scattering off a large polarised NH_3 target. The data, collected in the year 2007, cover the range $Q^2 > 1\,(\mathrm{GeV}/c)^2$, $0.004 < x < 0.7$ and improve the statistical precision of $g_1^p(x)$ by a factor of two in the region $x < 0.02$. The new proton asymmetries are combined with those previously published for the deuteron to extract the non-singlet spin-dependent structure function $g_1^{NS}(x, Q^2)$. The isovector quark density, $\Delta q_3(x, Q^2)$, is evaluated from a NLO QCD fit of g_1^{NS}. The first moment of Δq_3 is in good agreement with the value predicted by the Bjorken sum rule and corresponds to a ratio of the axial and vector coupling constants $|g_A/g_V| = 1.28 \pm 0.07(\mathrm{stat.}) \pm 0.10(\mathrm{syst.})$.

Keywords: COMPASS; Deep inelastic scattering; Spin; Structure function; QCD analysis; Bjorken sum rule

(To be Submitted to Physics Letters B)

COMPASS Collaboration

M.G. Alekseev[28], V.Yu. Alexakhin[7], Yu. Alexandrov[15], G.D. Alexeev[7], A. Amoroso[27], A. Austregesilo[10,17], B. Badełek[30], F. Balestra[27], J. Ball[22], J. Barth[4], G. Baum[1], Y. Bedfer[22], J. Bernhard[13], R. Bertini[27], M. Bettinelli[16], R. Birsa[24], J. Bisplinghoff[3], P. Bordalo[12,a], F. Bradamante[25], A. Bravar[24], A. Bressan[25], G. Brona[10,30], E. Burtin[22], M.P. Bussa[27], D. Chaberny[13], D. Čotić[13], M. Chiosso[27], S.U. Chung[17], A. Cicuttin[24,26], M. Colantoni[28], M.L. Crespo[24,26], S. Dalla Torre[24], S. Das[6], S.S. Dasgupta[6], O.Yu. Denisov[10,28], L. Dhara[6], V. Diaz[24,26], S.V. Donskov[21], N. Doshita[2,32], V. Duic[25], W. Dünnweber[16], A. Efremov[7], A. El Alaoui[22], P.D. Eversheim[3], W. Eyrich[8], M. Faessler[16], A. Ferrero[27,10], A. Filin[21], M. Finger[19], M. Finger jr.[7], H. Fischer[9], C. Franco[12], J.M. Friedrich[17], R. Garfagnini[27], F. Gautheron[1], O.P. Gavrichtchouk[7], R. Gazda[30], S. Gerassimov[15,17], R. Geyer[16], M. Giorgi[25], I. Gnesi[27], B. Gobbo[24], S. Goertz[2,4], S. Grabmüller[17], A. Grasso[27], B. Grube[17], R. Gushterski[7], A. Guskov[7], F. Haas[17], D. von Harrach[13], T. Hasegawa[14], F.H. Heinsius[9], R. Hermann[13], F. Herrmann[9], C. Heß[2], F. Hinterberger[3], N. Horikawa[18,c], Ch. Höppner[17], N. d'Hose[22], C. Ilgner[10,16], S. Ishimoto[18,d], O. Ivanov[7], Yu. Ivanshin[7], T. Iwata[32], R. Jahn[3], P. Jasinski[13], G. Jegou[22], R. Joosten[3], E. Kabuß[13], W. Käfer[9], D. Kang[9], B. Ketzer[17], G.V. Khaustov[21], Yu.A. Khokhlov[21], Yu. Kisselev[1,2], F. Klein[4], K. Klimaszewski[30], S. Koblitz[13], J.H. Koivuniemi[2], V.N. Kolosov[21], K. Kondo[2,32], K. Königsmann[9], R. Konopka[17], I. Konorov[15,17], V.F. Konstantinov[21], A. Korzenev[13,b], A.M. Kotzinian[7,22], O. Kouznetsov[7,22], K. Kowalik[30,22], M. Krämer[17], A. Kral[20], Z.V. Kroumchtein[7], R. Kuhn[17], F. Kunne[22], K. Kurek[30], L. Lauser[9], J.M. Le Goff[22], A.A. Lednev[21], A. Lehmann[8], S. Levorato[25], J. Lichtenstadt[23], T. Liska[20], A. Maggiora[28], M. Maggiora[27], A. Magnon[22], G.K. Mallot[10], A. Mann[17], C. Marchand[22], J. Marroncle[22], A. Martin[25], J. Marzec[31], F. Massmann[3], T. Matsuda[14], A.N. Maximov[7,+], W. Meyer[2], T. Michigami[32], Yu.V. Mikhailov[21], M.A. Moinester[23], A. Mutter[9,13], A. Nagaytsev[7], T. Nagel[17], J. Nassalski[30,+], T. Negrini[3], F. Nerling[9], S. Neubert[17], D. Neyret[22], V.I. Nikolaenko[21], A.G. Olshevsky[7], M. Ostrick[13], A. Padee[31], R. Panknin[4], D. Panzieri[29], B. Parsamyan[27], S. Paul[17], B. Pawlukiewicz-Kaminska[30], E. Perevalova[7], G. Pesaro[25], D.V. Peshekhonov[7], G. Piragino[27], S. Platchkov[22], J. Pochodzalla[13], J. Polak[11,25], V.A. Polyakov[21], G. Pontecorvo[7], J. Pretz[4], C. Quintans[12], J.-F. Rajotte[16], S. Ramos[12,a], V. Rapatsky[7], G. Reicherz[2], A. Richter[8], F. Robinet[22], E. Rocco[27], E. Rondio[30], D.I. Ryabchikov[21], V.D. Samoylenko[21], A. Sandacz[30], H. Santos[12,a], M.G. Sapozhnikov[7], S. Sarkar[6], I.A. Savin[7], G. Sbrizzai[25], P. Schiavon[25], C. Schill[9], L. Schmitt[17,e], T. Schlüter[16], S. Schopferer[9], W. Schröder[8], O.Yu. Shevchenko[7], H.-W. Siebert[13], L. Silva[12], L. Sinha[6], A.N. Sissakian[7], M. Slunecka[7], G.I. Smirnov[7], S. Sosio[27], F. Sozzi[25], A. Srnka[5], M. Stolarski[10], M. Sulc[11], R. Sulej[31], S. Takekawa[25], S. Tessaro[24], F. Tessarotto[24], A. Teufel[8], L.G. Tkatchev[7], S. Uhl[17], I. Uman[16], M. Virius[20], N.V. Vlassov[7], A. Vossen[9], Q. Weitzel[17], R. Windmolders[4], W. Wiślicki[30], H. Wollny[9], K. Zaremba[31], M. Zavertyaev[15], E. Zemlyanichkina[7], M. Ziembicki[31], J. Zhao[13,24], N. Zhuravlev[7] and A. Zvyagin[16]

[1] Universität Bielefeld, Fakultät für Physik, 33501 Bielefeld, Germany[f]
[2] Universität Bochum, Institut für Experimentalphysik, 44780 Bochum, Germany[f]
[3] Universität Bonn, Helmholtz-Institut für Strahlen- und Kernphysik, 53115 Bonn, Germany[f]
[4] Universität Bonn, Physikalisches Institut, 53115 Bonn, Germany[f]
[5] Institute of Scientific Instruments, AS CR, 61264 Brno, Czech Republic[g]
[6] Matrivani Institute of Experimental Research & Education, Calcutta-700 030, India[h]
[7] Joint Institute for Nuclear Research, 141980 Dubna, Moscow region, Russia
[8] Universität Erlangen–Nürnberg, Physikalisches Institut, 91054 Erlangen, Germany[f]
[9] Universität Freiburg, Physikalisches Institut, 79104 Freiburg, Germany[f]
[10] CERN, 1211 Geneva 23, Switzerland
[11] Technical University in Liberec, 46117 Liberec, Czech Republic[g]
[12] LIP, 1000-149 Lisbon, Portugal[i]
[13] Universität Mainz, Institut für Kernphysik, 55099 Mainz, Germany[f]
[14] University of Miyazaki, Miyazaki 889-2192, Japan[j]
[15] Lebedev Physical Institute, 119991 Moscow, Russia
[16] Ludwig-Maximilians-Universität München, Department für Physik, 80799 Munich, Germany[f,k]
[17] Technische Universität München, Physik Department, 85748 Garching, Germany[f,k]
[18] Nagoya University, 464 Nagoya, Japan[j]
[19] Charles University, Faculty of Mathematics and Physics, 18000 Prague, Czech Republic[g]
[20] Czech Technical University in Prague, 16636 Prague, Czech Republic[g]
[21] State Research Center of the Russian Federation, Institute for High Energy Physics, 142281 Protvino, Russia[l]
[22] CEA DAPNIA/SPhN Saclay, 91191 Gif-sur-Yvette, France
[23] Tel Aviv University, School of Physics and Astronomy, 69978 Tel Aviv, Israel[m]
[24] Trieste Section of INFN, 34127 Trieste, Italy
[25] University of Trieste, Department of Physics and Trieste Section of INFN, 34127 Trieste, Italy
[26] Abdus Salam ICTP and Trieste Section of INFN, 34127 Trieste, Italy
[27] University of Turin, Department of Physics and Torino Section of INFN, 10125 Turin, Italy
[28] Torino Section of INFN, 10125 Turin, Italy
[29] University of Eastern Piedmont, 1500 Alessandria, and Torino Section of INFN, 10125 Turin, Italy
[30] Sołtan Institute for Nuclear Studies and University of Warsaw, 00-681 Warsaw, Poland[n]
[31] Warsaw University of Technology, Institute of Radioelectronics, 00-665 Warsaw, Poland[o]
[32] Yamagata University, Yamagata, 992-8510 Japan[j]
[+] Deceased
[a] Also at IST, Universidade Técnica de Lisboa, Lisbon, Portugal
[b] On leave of absence from JINR Dubna
[c] Also at Chubu University, Kasugai, Aichi, 487-8501 Japan[j]
[d] Also at KEK, 1-1 Oho, Tsukuba, Ibaraki, 305-0801 Japan
[e] Also at GSI mbH, Planckstr. 1, D-64291 Darmstadt, Germany
[f] Supported by the German Bundesministerium für Bildung und Forschung
[g] Suppported by Czech Republic MEYS grants ME492 and LA242
[h] Supported by SAIL (CSR), Govt. of India
[i] Supported by the Portuguese FCT - Fundação para a Ciência e Tecnologia grants POCTI/FNU/49501/2002 and POCTI/FNU/50192/2003
[j] Supported by the MEXT and the JSPS under the Grants No.18002006, No.20540299 and No.18540281; Daiko Foundation and Yamada Foundation
[k] Supported by the DFG cluster of excellence ‘Origin and Structure of the Universe’ (www.universe-cluster.de)

In previous publications the COMPASS collaboration has presented new accurate values of the longitudinal spin asymmetry of the deuteron, A_1^d, covering a large range of x ($0.004 < x < 0.7$) in the region of deep inelastic scattering (DIS) $Q^2 > 1\,(\mathrm{GeV}/c)^2$ [1, 2]. These new values have led to an improved determination of the spin structure function $g_1^d(x, Q^2)$ in the low x region where only the SMC measurements existed before [3]. The first moment of $g_1^d(x)$ has also provided a more accurate value for the matrix element of the flavour singlet axial current $a_0 = 0.35 \pm 0.03(\mathrm{stat}) \pm 0.05(\mathrm{syst.})$ at $Q^2 = 3\,(\mathrm{GeV}/c)^2$, confirming the rather small contribution of the quark spins to the nucleon spin.

In this letter we present new COMPASS results for the inclusive double-spin asymmetry of the proton, A_1^p and for the spin structure function $g_1^p(x, Q^2)$ measured in the same kinematic range. In combination with the deuteron data, these results yield an evaluation of the isovector quark density, $\Delta q_3(x, Q^2) = \Delta u - \Delta d$, and its first moment which in turn provides a test of the Bjorken sum rule.

The proton data were collected in 2007 using a three target cell configuration and the upgraded COMPASS spectrometer, as described in [4]. The polarised target material is the ammonia previously used in the SMC experiment [5]. The polarisation was about 90% in absolute value, measured with a relative error of $\pm$ 2% [6]. The muon beam has a natural polarisation of about -80%. The energy of the incoming muons is constrained to be in the interval $140 < E_\mu < 180$ GeV and their polarisation is known with a relative precision of $\pm$ 5%. All events used in the present analysis are required to have a reconstructed primary interaction vertex (defined by the incoming and the scattered muon) inside one of the target cells. In order to cancel out the muon flux normalisation in the asymmetry calculation, incident muons are only accepted when their extrapolated trajectory crosses all three cells.

For most events the trigger is based on a combination of hodoscope signals defining the trajectory of the scattered muon. In addition to these "inclusive triggers", low x events are also selected by an additional condition on the energy deposit in the hadron calorimeter, which is then used as a "semi-inclusive trigger". At large x and Q^2 most events are selected by conditions on the calorimeter signal only, without any input from hodoscopes. For this "calorimeter-only trigger" as well as for the semi-inclusive one, the presence of a reconstructed hadron trajectory compatible with the calorimeter information is required.

The kinematic region is defined by requiring the photon virtuality $Q^2 > 1\,(\mathrm{GeV}/c)^2$ and the fractional energy y transfered from the beam muon to the virtual photon to be between 0.1 and 0.9. The region which is most affected by radiative corrections is eliminated by the cut $y < 0.9$. The total sample after all cuts amounts to 85.3 million events.

The longitudinal virtual-photon proton asymmetry, A_1^p, is evaluated from the numbers of events collected in the different target cells by the method used in our previous analyses of deuteron data [1, 2]. Neighbouring target cells are polarised in opposite directions and data from both target spin orientations are thus recorded simultaneously. The lengths of the cells are chosen so that the two samples collected with opposite spin orientations have in average the same acceptance, which limits the risk of false asymmetries. The target spin directions are reversed once per day by rotating the magnetic field and a few times per year by changing the microwave frequencies used for dynamic nuclear polarisation. The asymmetries are calculated from the numbers of events in cells with opposite spin orientations collected before and after a

[l] Supported by Supported by CERN-RFBR grant 08-02-91009
[m] Supported by the Israel Science Foundation, founded by the Israel Academy of Sciences and Humanities
[n] Supported by Ministry of Science and Higher Education grant 41/N-CERN/2007/0
[o] Supported by KBN grant nr 134/E-365/SPUB-M/CERN/P-03/DZ299/2000

field rotation so that flux and acceptance factors cancel out.

Radiative corrections are applied separately to the asymmetries obtained for the inclusive triggers and to those obtained for the semi-inclusive and calorimeter-only triggers because radiative elastic events contribute only to the former ones. Another correction is applied to account for the polarisation of the ^{14}N nucleus. For this spin 1 object the correction is proportional to $A_1^d(x)$ and affected by factors accounting for the number of ^{14}N nuclei vs. H atoms, the alignment of the proton spin vs. the ^{14}N spin and the ratio of ^{14}N to H polarisations [7]:

$$\Delta A_1^p(x) = \frac{1}{3} \cdot (-\frac{1}{3}) \cdot \frac{1}{6} \cdot \frac{\sigma_d(x)}{\sigma_p(x)} \cdot A_1^d(x). \tag{1}$$

The corrections for the various intervals of x are given in the appendix. They are of the order of 0.01 for $x > 0.35$ and are mainly important for the evaluation of the first moment of the spin structure function $\Gamma_1^p(Q^2) = \int_0^1 g_1^p(x, Q^2)dx$.

The target dilution factor is given by the ratio of the cross-section for the polarisable protons to that of all nuclei in a target cell. The values for the NH_3 target are shown in Fig. 1 as a function of x, for inclusive and hadron triggers. They are about 14% in the medium x region, with a rise at large x due to the reduced cross section on heavy targets in this region, and a drop at low x for inclusive triggers due to the contribution of radiative elastic events on the proton.

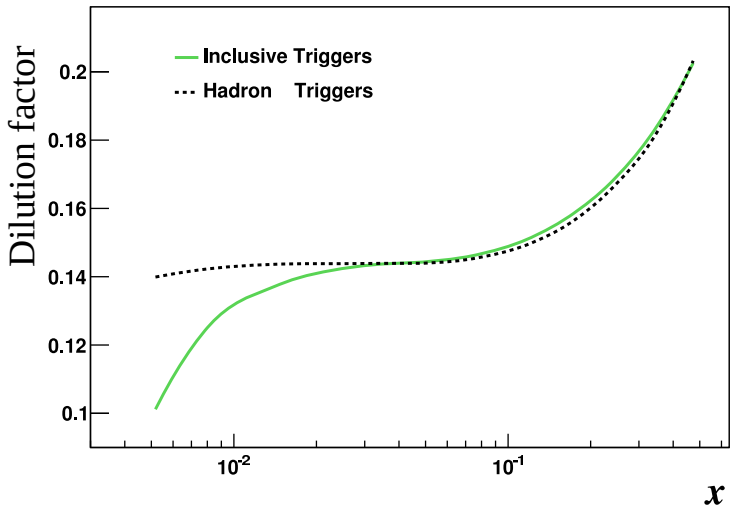

Figure 1: The dilution factor f of the NH_3 polarised target as a function of x for inclusive and hadron triggers [3]. The values of $f(x)$ are averaged over the Q^2 range of the corresponding triggers.

The new values of $A_1^p(x)$ are shown in Fig. 2 in comparison with results from previous experiments. The Q^2 of different points at any fixed value of x varies considerably since the incident energy of the various experiments ranges from 6 to 200 GeV. The fact that all results align reasonably well on a single curve illustrates the well known observation that the Q^2 dependence of A_1^p is very weak in the DIS region. This is further illustrated in Fig. 3 which shows $A_1^p(x, Q^2)$ as a function of Q^2 for the COMPASS data. No significant Q^2 dependence is observed in any interval of x.

The systematic errors of the COMPASS results for A_1^p are shown by the band at the bottom of Fig. 2 and listed in Table 1. They contain the contributions due to the uncertainties on the target polarisation, the beam polarisation, the dilution factor and the ratio $R = \sigma_L/\sigma_T$ [8] used in the depolarisation factor, which are equal to 2, 5, 1 and at most 3%, respectively. Combined in quadrature, these uncertainties amount to a systematic error of at most 6% of

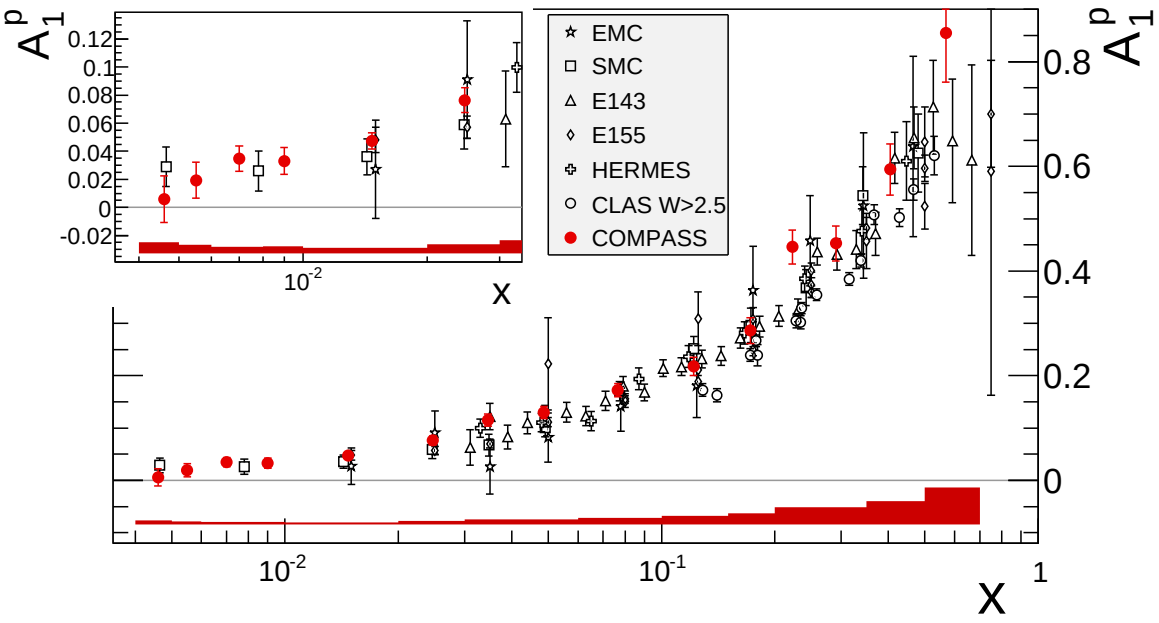

Figure 2: The asymmetry $A_1^p(x)$ as measured by COMPASS and previous results from EMC [9], SMC [3], HERMES [10], SLAC E143 [11], E155 [12] and CLAS [13] at $Q^2 > 1\,(\mathrm{GeV}/c)^2$. The cut $W > 2.5$ GeV has been applied to select DIS events in the CLAS data. Only statistical errors are shown with the data points. The band at the bottom shows the estimated size of the systematic errors for the COMPASS data.

the quoted value. The error due to the neglect of the transverse asymmetry, A_2^p, is less than 0.002 in the full range of x. Another possible contribution to the systematic error is due to false asymmetries generated by instabilities in some components of the spectrometer. Such effects have been searched for in faked configurations, where the physics asymmetry does not contribute, and were found to be compatible with zero. The comparison of results obtained with opposite orientations of the target field also does not show any significant difference. The possible error due to false asymmetries has been estimated by a statistical test performed on the distribution of asymmetries extracted from 46 subsamples. Time-dependent effects which would lead to a broadening of these distributions were not observed. As a consequence the limit $\sigma_{syst} < 0.47\sigma_{stat}$ was obtained at the level of one standard deviation. The different contributions to the systematic error are summarised in Table 2.

The longitudinal spin structure function g_1^p of the proton is obtained from A_1^p by the relation

$$g_1^p = \frac{F_2^p}{2x(1+R)} A_1^p \tag{2}$$

where F_2^p is the spin independent structure function. The values obtained with the SMC parameterisation of the world data on F_2^p [3] and the parameterisation of R already used in the depolarisation factor are listed in Table 1 with their statistical and systematic errors. They are also shown in Fig. 4 in comparison with the SMC values. It can be seen that the COMPASS data improve the statistical precision at least by a factor of two in the low x region, covered only by the two experiments shown here. The new data points are compatible with a constant $g_1^p(x)$ for $0.004 < x < 0.04$ and do not show evidence either for an increase or a decrease when $x \to 0$. This observation remains valid when the data points are moved to a common Q^2 according to the fits quoted in Ref. [2] and the constant value is found to be $g_1^p = 0.48 \pm 0.03(\mathrm{stat.}) \pm 0.04(\mathrm{syst.})$ at $Q^2 = 3(\mathrm{GeV}/c)^2$.

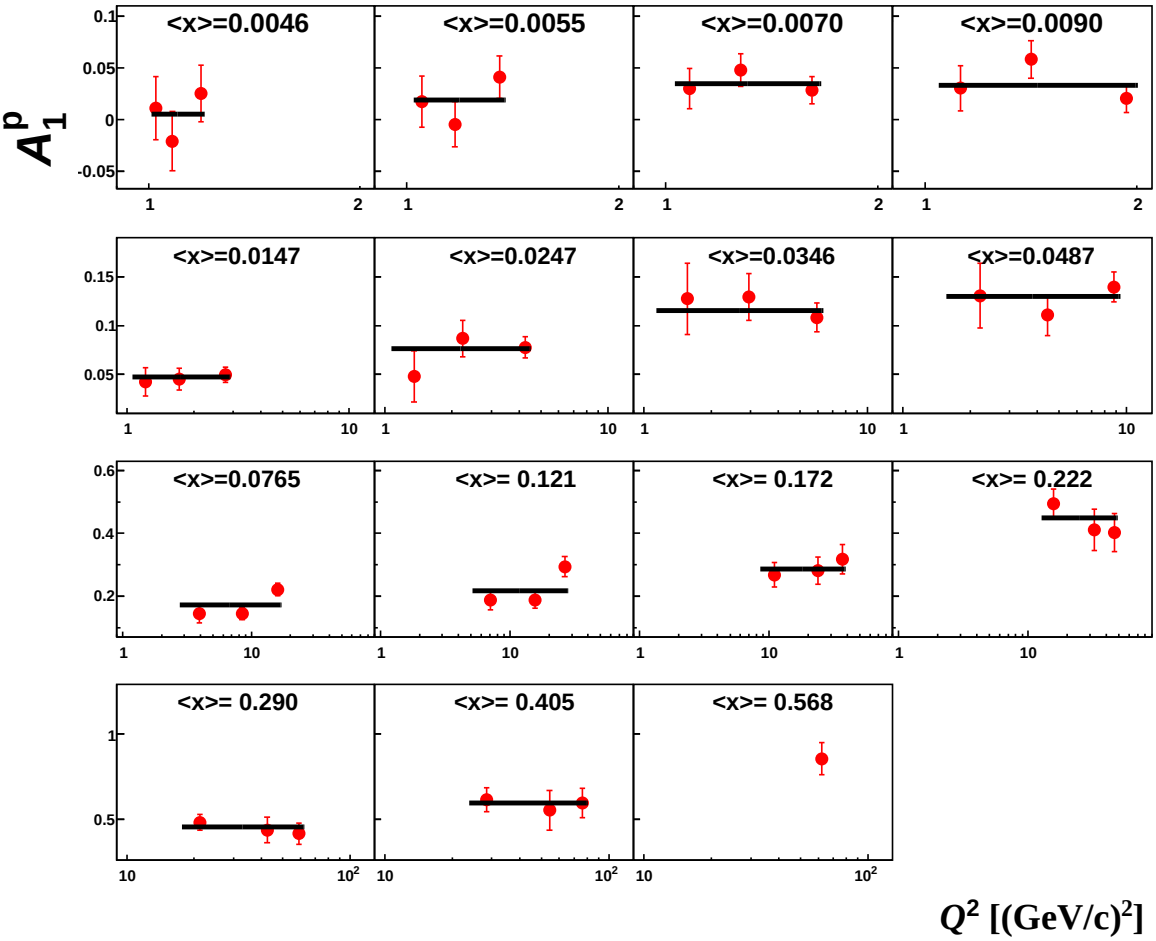

Figure 3: Values of A_1^p as a function of Q^2 in intervals of x. The errors are statistical only. The solid lines show the results of fits to a constant.

The non-singlet spin structure function

$$g_1^{NS}(x,Q^2) = g_1^p(x,Q^2) - g_1^n(x,Q^2) \tag{3}$$

is of special interest because its Q^2 dependence is decoupled from the singlet and the gluon spin densities:

$$g_1^{NS}(x,Q^2) = \frac{1}{6}\int_x^1 \frac{dx'}{x'} C^{NS}\left(\frac{x}{x'}, \alpha_s(Q^2)\right)\Delta q_3(x',Q^2) \tag{4}$$

where C^{NS} is a Wilson coefficient function and Δq_3 the isovector spin density. Consequently a fit of the Q^2 evolution of g_1^{NS} requires only a small number of parameters to describe the shape of $\Delta q_3(x)$ at some reference Q^2. According to the Bjorken sum rule the integral of g_1^{NS} at any fixed Q^2 is proportional to the ratio g_A/g_V of the axial and vector coupling constants and given by the relation

$$\Gamma_1^{NS}(Q^2) = \frac{1}{6}\left|\frac{g_A}{g_V}\right| C_1^{NS}(Q^2) \tag{5}$$

where the non-singlet coefficient function $C_1^{NS}(Q^2)$ has been calculated in perturbative QCD up to the third order in $\alpha_s(Q^2)$ [14]. The comparison of the value of $|g_A/g_V|$ obtained from the data with the one derived from neutron β decay ($|g_A/g_V| = 1.2694 \pm 0.0028$ [15]) thus provides a test of the Bjorken sum rule, free of systematic errors arising from uncertainties on the gluon helicity distribution.

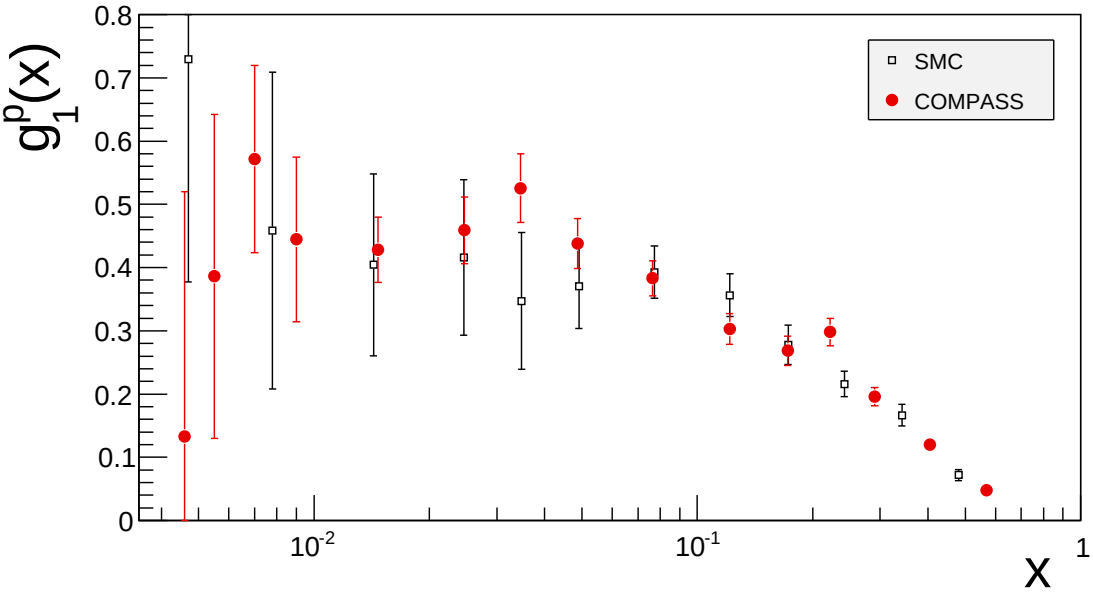

Figure 4: The spin structure function $g_1^p(x, Q^2)$ vs. x as measured by COMPASS at the Q^2 of each measured point. Previous results from SMC [3] are shown for comparison. The errors are statistical only.

In the present analysis, the values of g_1^{NS} are obtained as

$$g_1^{NS}(x, Q^2) = 2\left[g_1^p(x, Q^2) - \frac{g_1^d(x, Q^2)}{1 - 1.5\omega_D}\right] \tag{6}$$

where the values of g_1^d are taken from Ref. [2] and the deuteron D-state probability, ω_D, is 0.05 ± 0.01 [16].

The proton and deuteron data have been obtained at the same (x, Q^2) points, which avoids the need of interpolation. A correction has however to be applied to the deuteron data for the admixtures of ^{7}Li and ^{1}H in the ^{6}LiD target material, which was not taken into account in Ref. [2]. The ratios of isotopes ^{7}Li/^{6}Li and H/D were found to be 4.4 % and 0.5 % respectively [17] and ^{7}Li and ^{1}H are both polarised at more than 90% [18]. The resulting corrections to A_1^d are given in the appendix. They are negligible at low x but reach 0.015 at $x = 0.50$ and reduce the first moment Γ_1^d by 0.002.

In the present analysis, $Q^2 = 3\,(\mathrm{GeV}/c)^2$ has been taken as reference Q^2 and the following parameterisation has been used for Δq_3:

$$\Delta q_3(x) = \eta_3 \frac{x^{\alpha_3}(1-x)^{\beta_3}}{\int_0^1 x^{\alpha_3}(1-x)^{\beta_3} dx}\,. \tag{7}$$

As for our previous analysis [2] the QCD fit at NLO of the COMPASS values of g_1^{NS} to Eq.(4) has been performed with two different programs, the first one working in the (x,Q^2) space [19], the second one in the space of moments [20]. Both programs give the same values of the fitted parameters and similar χ^2-probabilities. The fitted parameters obtained are listed in Table 3. The exponent α_3 is in the range of Regge pole predictions [21] and the integral η_3 is in excellent agreement with the Bjorken sum rule prediction $|g_A/g_V|$. The fitted distribution of $xg_1^{NS}(x)$ and the data points moved to the reference Q^2 are shown in Fig. 5 (left).

The integral of g_1^{NS} has also been evaluated from the measured values in the range $0.004 < x < 0.7$ with additional low and high x contributions taken from the fit (Table 4).

x range	$\langle x \rangle$	$\langle Q^2 \rangle$ [$(\mathrm{GeV}/c)^2$]	A_1^p	g_1^p
0.004 - 0.005	0.0046	1.10	$0.006 \pm 0.017 \pm 0.008$	$0.133 \pm 0.389 \pm 0.183$
0.005 - 0.006	0.0055	1.20	$0.019 \pm 0.013 \pm 0.006$	$0.385 \pm 0.256 \pm 0.123$
0.006 - 0.008	0.0070	1.37	$0.035 \pm 0.009 \pm 0.005$	$0.571 \pm 0.147 \pm 0.079$
0.008 - 0.010	0.0090	1.59	$0.033 \pm 0.010 \pm 0.005$	$0.445 \pm 0.130 \pm 0.067$
0.010 - 0.020	0.0147	2.14	$0.047 \pm 0.006 \pm 0.004$	$0.427 \pm 0.052 \pm 0.036$
0.020 - 0.030	0.0247	3.24	$0.076 \pm 0.009 \pm 0.006$	$0.459 \pm 0.053 \pm 0.037$
0.030 - 0.040	0.0346	4.36	$0.115 \pm 0.012 \pm 0.009$	$0.525 \pm 0.054 \pm 0.041$
0.040 - 0.060	0.0487	6.05	$0.130 \pm 0.012 \pm 0.010$	$0.438 \pm 0.039 \pm 0.032$
0.060 - 0.100	0.0765	9.42	$0.172 \pm 0.013 \pm 0.012$	$0.383 \pm 0.028 \pm 0.026$
0.100 - 0.150	0.122	14.9	$0.218 \pm 0.017 \pm 0.015$	$0.303 \pm 0.024 \pm 0.021$
0.150 - 0.200	0.172	20.9	$0.286 \pm 0.024 \pm 0.020$	$0.268 \pm 0.023 \pm 0.019$
0.200 - 0.250	0.222	26.7	$0.446 \pm 0.032 \pm 0.030$	$0.298 \pm 0.022 \pm 0.020$
0.250 - 0.350	0.290	34.6	$0.453 \pm 0.033 \pm 0.032$	$0.196 \pm 0.014 \pm 0.013$
0.350 - 0.500	0.405	47.1	$0.594 \pm 0.049 \pm 0.043$	$0.120 \pm 0.010 \pm 0.008$
0.500 - 0.700	0.568	62.1	$0.855 \pm 0.094 \pm 0.068$	$0.048 \pm 0.005 \pm 0.004$

Table 1: Values of A_1^p and g_1^p as a function of x with the corresponding average value of Q^2. The first error is statistical, the second one systematical.

Beam polarisation	$\Delta P_b/P_b$	$0.04/0.8 = 5.0\%$
Target polarisation	$\Delta P_t/P_t$	2%
Depolarisation factor	$\Delta D(R)/D(R)$	2.0 – 3.0 %
Dilution factor	$\Delta f/f$	1 %
Total	ΔA_1^{mult}	$\simeq 0.06 A_1$
Transverse asymmetry	$\eta \cdot A_2$	$< 2.0 \times 10^{-3}$
Rad. corrections	ΔA_1^{RC}	$10^{-4} - 10^{-3}$
False asymmetry	A_{false}	$< 0.47 \cdot \Delta A_1^{stat}$

Table 2: Decomposition of the systematic error of A_1^p into multiplicative (top) and additive (bottom) contributions.

It is observed that about 92% of the first moment Γ_1^{NS} comes from the measured region. The dependence of the first moment of g_1^{NS} on its lower limit is shown in Fig. 5 (right). As already observed in the HERMES analysis [10], the integral does not saturate at $x \approx 0.01 - 0.02$ while the value obtained at the lowest x accessible in the present analysis (0.180 ± 0.009) is less than one standard deviation below the value expected from the Bjorken sum rule (0.188). The value of $|g_A/g_V|$ derived from the value of Γ_1^{NS} by Eq.(5) is identical to the one obtained from the fit and confirms the validity of the Bjorken sum rule with a statistical precision of 5%.

The dominant systematic error on this result is due to the uncertainty of 5% on the beam polarisation, which is common to the proton and deuteron data and therefore translates directly into a 5% error on $|g_A/g_V|$. Other contributions due to the target polarisation and the dilution factor are estimated to be ± 0.04 and ± 0.06 for the proton and deuteron terms, respectively. The resulting systematic error is ± 0.10. The errors related to the fit or to the evolution of the data to a common Q^2 are found to be negligible. In particular, it was checked that the same value of g_A/g_V is obtained when the reference Q^2 is 1.0, 3.0 or 10.0 $(\mathrm{GeV}/c)^2$ although the exponent

Param.	Value
η_3	1.28 ± 0.07
α_3	-0.22 ± 0.07
β_3	$2.2 \pm^{0.5}_{0.4}$
χ^2/ND	14.4/12
Prob.	0.27

Table 3: Results of the fits of $\Delta q_3(x)$ at $Q^2 = 3\,(\mathrm{GeV}/c)^2$.

x range	Γ_1^{NS}
0 – 0.004	0.0098
0.004 – 0.7	$0.175 \pm 0.009 \pm 0.015$
0.7 – 1.0	0.0048
0 – 1	$0.190 \pm 0.009 \pm 0.015$

Table 4: First moment Γ_1^{NS} at $Q^2 = 3\,(\mathrm{GeV}/c)^2$ from the COMPASS data points. The contributions from the unmeasured regions are estimated from the NLO fit to g_1^{NS}; their errors are negligible.

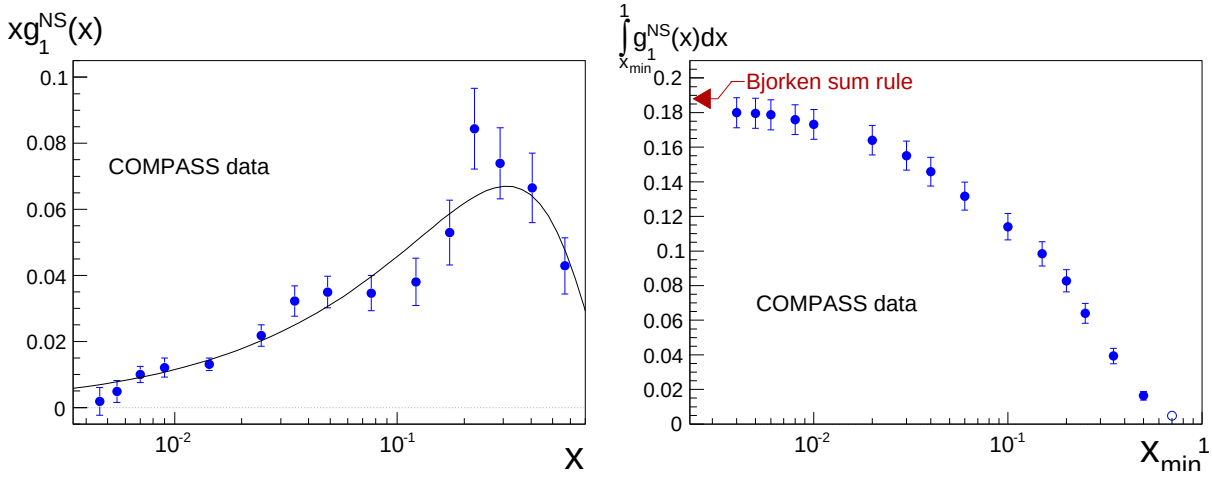

Figure 5: Left: Values of $g_1^{NS}(x)$ at $Q^2 = 3\,(\mathrm{GeV}/c)^2$, derived from the COMPASS measurements of A_1^p and A_1^d and result of a three parameter QCD fit at NLO. The errors are statistical only. Right: $\int_{x_{min}}^1 g_1^{NS} dx$ as a function of x_{min} as obtained from the COMPASS data points. The open circle at $x = 0.7$ is obtained from the fit. The arrow on the left side shows the value expected for the full range $0 < x < 1$ with $|g_A/g_V| = 1.269$ [15].

α_3 varies from -0.15 to -0.28 when Q^2 is moved from 1 to 10 and the shape of $g_1^{NS}(x)$ thus becomes quite different.

The test of the Bjorken sum rule performed in the present analysis of the COMPASS proton and deuteron data is thus mainly limited by systematics:

$$|g_A/g_V| = 1.28 \pm 0.07(\mathrm{stat.}) \pm 0.10(\mathrm{syst.}), \tag{8}$$

to be compared with the value 1.2694 ± 0.0028 derived from neutron β decay [15].
The COMPASS value of $\Gamma_1^{NS}$is in good agreement with the one obtained by the SMC (0.198 ± 0.023 at Q^2 = 10 $(\mathrm{GeV}/c)^2$) [3] and improves the statistical precision by a factor 2.5. The cumulative integral of g_1^{NS} truncated at $x_{min} = 0.021$ is equal to $0.1583 \pm 0.0085(\mathrm{stat.}) \pm 0.014(\mathrm{syst.})$, in good agreement with the HERMES value of $0.1484 \pm 0.0055(\mathrm{stat.}) \pm 0.016(\mathrm{syst.})$ obtained at Q^2 = 5 $(\mathrm{GeV}/c)^2$ [10].

In conclusion, the COMPASS collaboration has performed new measurements of the longitudinal spin asymmetry of the proton, covering a large range of x ($0.004 < x < 0.7$) in the DIS region, $Q^2 > 1(\mathrm{GeV}/c)^2$. The new data improve the statistical precision in the low x region by a factor of 2–3 and show no evidence either for an increase or a decrease of the spin structure function g_1^p in this region. In combination with the previously published results on the deuteron, the new data improve the evaluation of the non-singlet spin structure function g_1^{NS} and provide

a test of the Bjorken sum rule, which is satisfied within one standard deviation of the statistical uncertainty.

Acknowledgements

We gratefully acknowledge the support of the CERN management and staff and the skill and effort of the technicians of our collaborating institutes. Special thanks go to V. Anosov and V. Pesaro for their technical support during the installation and the running of this experiment. This work was made possible thanks to the financial support of our funding agencies.

Appendix

x range	Corr. to A_1^p	Corr. to A_1^d
0.004 - 0.005	0.000	0.000
0.005 - 0.006	0.000	0.000
0.006 - 0.008	0.000	0.001
0.008 - 0.010	0.000	0.001
0.010 - 0.020	0.000	0.001
0.020 - 0.030	0.000	0.001
0.030 - 0.040	-0.000	0.002
0.040 - 0.060	-0.001	0.002
0.060 - 0.100	-0.001	0.003
0.100 - 0.150	-0.003	0.004
0.150 - 0.200	-0.004	0.006
0.200 - 0.250	-0.005	0.008
0.250 - 0.350	-0.006	0.010
0.350 - 0.500	-0.009	0.013
0.500 - 0.700	-0.014	0.017

Table 5: Corrections to the COMPASS spin asymmetries A_1^p and A_1^d due to the the ^{14}N polarisation and to the admixture of ^{7}Li and ^{1}H into the ^{6}LiD target material. In both cases the correction must be subtracted from the measured asymmetries. The corrections to A_1^p are already applied to the values quoted in the present letter.

References

[1] COMPASS Collaboration, E. S. Ageev *et al.*, Phys. Lett. B **612** (2005) 154.
[2] COMPASS Collaboration, V. Yu. Alexakhin *et al.*, Phys. Lett. B **647** (2007) 8.
[3] SMC, B. Adeva *et al.*, Phys. Rev. D **58** (1998) 112001.
[4] COMPASS Collaboration, M. Alekseev *et al.*, Phys. Lett. B **680** (2009) 217.
[5] SMC, B. Adeva *et al.*, Phys. Lett. B **412** (1997) 414.
[6] Yu. Kisselev *et al.*, "Spin Interactions in Ammonia and Methods to Cross-check Polarisation", Spin Praha 08, Advanced Studies Institute, Symmetries and Spin, July 20-26,2008.
[7] O. A. Rondon, Phys. Rev. C **60** (1999) 035201.
[8] E143 Collaboration, K. Abe *et al.*, Phys. Lett. B **452** (1999) 194.
[9] EMC, J. Ashman *et al.*, Phys. Lett. B **206** (1988) 364; Nucl. Phys. B **328** (1989) 1.
[10] HERMES Collaboration, A. Airapetian *et al.*, Phys. Rev. D **75** (2007) 012007.
[11] E143 Collaboration, K. Abe *et al.*, Phys. Rev. D **58** (1998) 112003.
[12] E155 Collaboration, P. L. Anthony *et al.*, Phys. Lett. B **493** (2000) 19.

[13] CLAS Collaboration, K. V. Dharmawardane *et al.*, Phys. Lett. B **641** (2006) 11.
[14] S. A. Larin, T. van Ritbergen and J. A. M. Vermaseren, Phys. Lett. B **404** (1997) 153.
[15] C. Amsler *et al.* (Particle Data Group), Phys. Lett. B **667** (2008) 1.
[16] R. Machleidt, K. Holinde and C. Elster, Phys. Rep. **149** (1987) 1.
[17] S. Neliba *et al.*, Nucl. Instrum. Meth. A **526** (2004) 144.
[18] J. Ball *et al.*, Nucl. Instrum. Meth. A **498** (2003) 101.
[19] SMC, B. Adeva *et al.*, Phys. Rev. D **58** (1998) 112002.
[20] A. N. Sissakian, O. Yu. Shevchenko and O. N. Ivanov, Phys. Rev. D **70** (2004) 074032.
[21] S. D. Bass, Mod. Phys. Lett. A **22** (2007) 1005.